

# PMC-Patients: A Large-scale Dataset of Patient Notes and Relations Extracted from Case Reports in PubMed Central

Zhengyun Zhao<sup>1\*</sup>, Qiao Jin<sup>2\*</sup>, Sheng Yu<sup>1†</sup>

<sup>1</sup> Center for Statistical Science, Tsinghua University

<sup>2</sup> School of Medicine, Tsinghua University

{zhengyun21, jqal4}@mails.tsinghua.edu.cn

syu@tsinghua.edu.cn

## Abstract

We present PMC-Patients, a dataset consisting of 167k patient notes with 3.1M relevant article annotations and 293k similar patient annotations. The patient notes are extracted by identifying certain sections from case reports in PubMed Central, and those with at least CC BY-NC-SA license are re-distributed. Patient-article relevance and patient-patient similarity are defined by citation relationships in PubMed. We also perform four tasks with PMC-Patients to demonstrate its utility, including Patient Note Recognition, Patient-Patient Similarity, Patient-Patient Retrieval, and Patient-Article Retrieval. In summary, PMC-Patients provides the largest-scale patient notes with high quality, diverse conditions, easy access, and rich annotations<sup>1</sup>.

## 1 Introduction

Recent Natural Language Processing (NLP) models have shown great successes in a variety of tasks (Devlin et al., 2019; Brown et al., 2020), such as text classification, information extraction and retrieval, question answering, and summarization. They provide promising opportunities for the development of clinical decision support systems (Garg et al., 2005; Kawamoto et al., 2005), which automatically analyze Electronic Health Records (EHR) of patients and assist clinical decision making.

Data unavailability due to privacy concerns is one of the biggest challenges in clinical NLP (Chapman et al., 2011), and about half of the studies surveyed in a recent review used private datasets (Wu et al., 2020), causing reproduction issues. Only a few patient note datasets are publicly available (Styler et al., 2014; Johnson et al., 2016; Caufield et al., 2018), most of which are small-scale. MIMIC-III (Johnson et al., 2016), an EHR

dataset, is the most notable example and has been widely used for various purposes (Komorowski et al., 2018; Mullenbach et al., 2018; Alsentzer et al., 2019; Huang et al., 2019). However, it only includes 46.1k patients in critical care departments without relational annotations, and the data quality is questionable (Kurniati et al., 2019). An ideal patient note dataset should be large-scale, high-quality, cover diverse medical conditions, and have rich annotations to perform downstream tasks.

In this paper, we collect such a patient note dataset from case reports in PubMed Central (PMC). “Case report” is a specific type of medical publication, which typically consists of 1. a patient note that summarizes the patient’s whole admission, progress, discharge, and follow-up situations; and 2. a literature review of similar cases and relevant articles. We extract the patient notes by identifying certain sections and consider scientific articles and other case reports in the references to be relevant and similar, respectively. An overview of the PMC-Patients is shown in Figure 1.

In summary, PMC-Patients is: 1. **publicly available**: the whole dataset can be easily downloaded; 2. **large-scale**: PMC-Patients has the largest scale with 167k patients, and more can be extracted with distant supervision; 3. **high-quality**: the patient notes are of publication-quality; 4. **diverse**: PMC-Patients covers a variety of medical conditions; 5. **annotated**: Patient notes are annotated with relevant articles and similar notes. The dataset collection procedure and characteristics will be introduced in Section 2 and Section 3, respectively.

PMC-Patients can be used for various purposes, such as case report literature mining (Karami et al. 2019), pre-training clinical language models (Alsentzer et al. 2019), and building downstream tasks. In this paper, we explore Patient Note Recognition, Patient-Patient Similarity, Patient-Patient Retrieval, and Patient-Article Retrieval using PMC-Patients, which will be described in Section 4-7.

\*Equal contribution.

†Corresponding author.

<sup>1</sup>The dataset and code are available at <https://github.com/zhao-zyl5/PMC-Patients>.

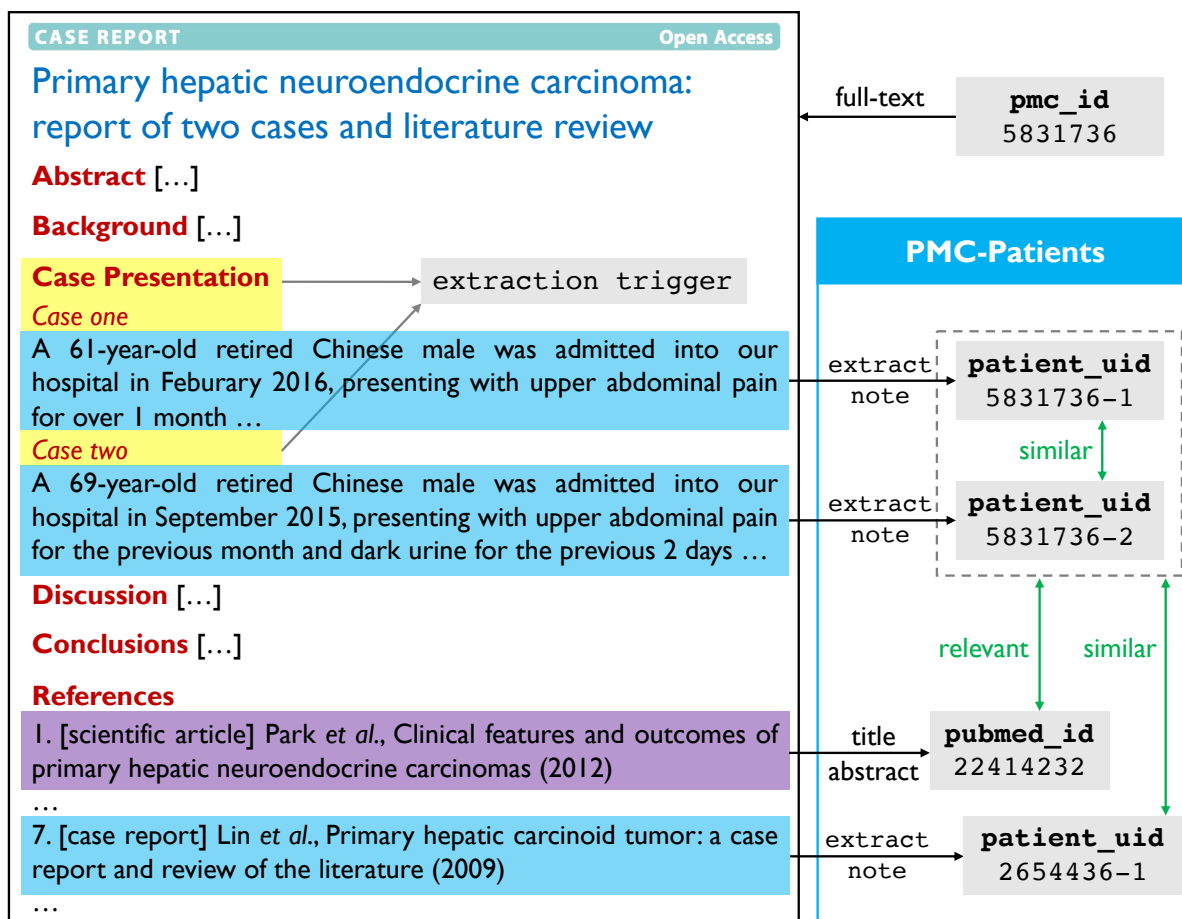


Figure 1: Overview of the PMC-Patients dataset architecture. Patient notes are extracted by identifying certain section names in PMC articles. The cited articles and case reports are considered relevant and similar, respectively. Patients from the same report are also considered similar.

## 2 Dataset Collection

### 2.1 Data Source

PubMed Central (PMC)<sup>2</sup> is a free full-text archive of biomedical and life sciences journal literature, currently archiving 7.6M articles. As a subset of PMC, PMC Open Access (OA)<sup>3</sup> includes over 4M articles available for reusing, though with various licenses and some are not allowed for redistribution. Therefore, only publications with at least CC BY-NC-SA license<sup>4</sup>, which amount to nearly 3.2M, are used to build PMC-Patients.

Relational annotations are defined by citation relationships in PubMed<sup>5</sup>. Publications without titles or abstracts are excluded.

<sup>2</sup><https://www.ncbi.nlm.nih.gov/pmc/>

<sup>3</sup><https://www.ncbi.nlm.nih.gov/pmc/tools/openftlist/>

<sup>4</sup><https://creativecommons.org/licenses/by-nc-sa/4.0/>

<sup>5</sup><https://pubmed.ncbi.nlm.nih.gov/>

### 2.2 Collection Pipeline

The collection pipeline of PMC-Patients is shown in Figure 2, which can be summarized as follows:

- For each section of each article, identify whether there are potential patient notes with **extraction triggers**.
- For sections triggering in step 1, extract patient note candidates with **extractors**.
- Apply various **filters** to candidates to exclude non-patient-notes.
- Relational annotations** are defined by citation relationships in PubMed.

#### (a) Extraction Triggers

Extraction triggers are a set of regular expressions to identify whether there is no, one or multiple potential patient notes in a given section, basically consisting of two successive triggers:

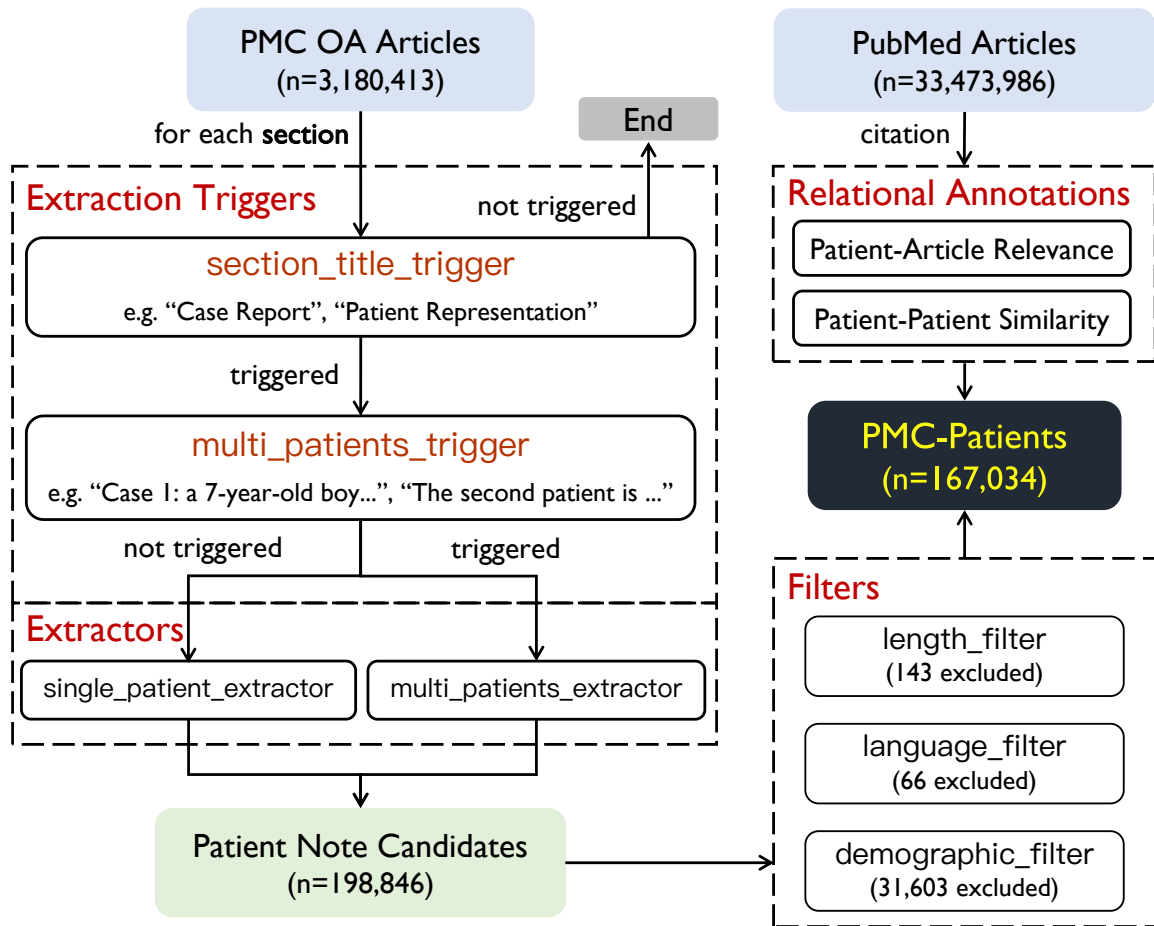


Figure 2: Collection pipeline of PMC-Patients. Patient notes are identified by **extraction triggers**, extracted by **extractors** and pass various **filters**. **Relational annotations** are defined by citation relationships in PubMed.

`section_title_trigger`: Searching in the **section title** for certain phrases that indicate the presence of patient notes, such as “Case Report” and “Patient Representation”.

`multi_patients_trigger`: Searching for certain patterns in the first sentence of each **paragraph** and titles of **subsections** to identify whether multiple notes are presented, such as “The second patient” and “Case 1”.

### (b) Extractors

Extracting is performed at paragraph level. Depending on whether `multi_patients_trigger` is triggered, different extractors are used:

`single_patient_extractor`: Extract all paragraphs in the section as one note, if not triggered.

`multi_patients_extractor`: Extract paragraphs between successive triggering parts (the last one is taken till the end of the section) as multiple patient notes, if triggered.

### (c) Filters

We remove noisy candidates with three filters:

`length_filter`: Candidates with less than 10 words are excluded.

`language_filter`: Candidates with more than 3% non-English characters are excluded.

`demographic_filter`: The age and gender of a patient are identified using regular expressions. Candidates missing either demographic characteristic are excluded.

### (d) Relational annotations

Two types of relations are annotated:

*Patient-Article Relevance*: All articles citing or cited by the article containing a patient note, plus the article itself, are defined as relevant articles to the patient.

*Patient-Patient Similarity*: Patients extracted from the relevant articles to a patient are defined as similar patients to the given patient with a similarity of 1, and patients from the same article are annotated with a similarity of 2.

## 2.3 Dataset Quality Evaluation

To evaluate the quality of the automatically extracted patient notes and demographics, we randomly sample 500 articles with at least one extracted case for human annotations. Two independent biomedical experts (senior M.D. candidates) are employed to label the patient note spans and their demographics in these articles. Agreed annotations are directly considered as the ground truth. Disagreed annotations will be discussed in the second round, and the final agreement will be used as the ground truth.

The extraction quality of PMC-Patients and the two experts are shown in Table 1. The results show that the patient note spans extracted in PMC-Patients are of high quality with a larger than 90% strict F1 score, which will be discussed more in Section 4. In addition, the extracted demographics are close to 100% correct.

Quality	Note Span	Age	Gender
PMC-Patients	91.24	99.77	100.0
Expert A	97.34	100.0	100.0
Expert B	97.28	99.91	99.49

Table 1: Extraction quality of the PMC-Patients dataset and two experts (in percentages). Note span recognition is evaluated by F1 score. Age recognition is evaluated by  $\min(\text{annotated\_age}, \text{true\_age}) / \max(\text{annotated\_age}, \text{true\_age})$ . Gender recognition is evaluated by accuracy.

## 3 Dataset Characteristics

### 3.1 Basic Statistics

Table 2 reports basic statistics of PMC-Patients, MIMIC-III, and MIMIC discharge summaries, the note type most similar to PMC-Patients in MIMIC. PMC-Patients have  $3.5\times$  patients as MIMIC, and  $2.8\times$  notes as MIMIC discharge summaries.

On average, PMC-Patients notes (410 words) are longer than MIMIC (223 words), but shorter than discharge summaries (1282 words). Figure 3 presents the length distributions of PMC-Patients, MIMIC and discharge summaries in MIMIC. Lengths of notes in PMC-Patients are approximately normally distributed, while discharge summaries in MIMIC present almost a uniform distribution. With various note types of different structures mixing, the length distribution of all notes in MIMIC has two peaks.

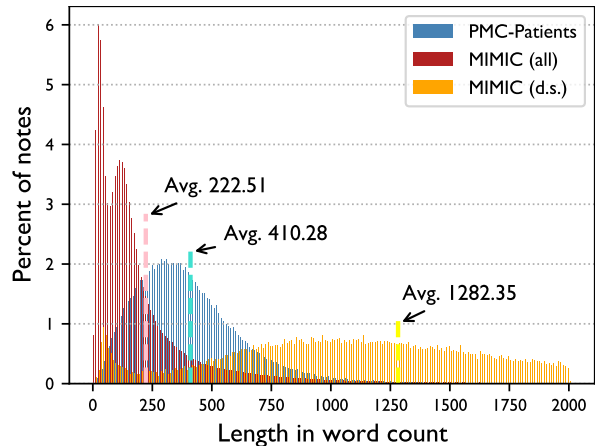


Figure 3: Length distributions of PMC-Patients compared to MIMIC-III and MIMIC discharge summaries (x-axis truncated).

### 3.2 Patient Analysis

**Demographics** We show the age distribution of PMC-Patients in comparison to MIMIC-III in Figure 4. On average, patients in PMC-Patients are younger than MIMIC-III (43.40 v.s. 55.19 years old), and patient ages are more evenly distributed (6.49 v.s. 5.70 Shannon bits). PMC-Patients consists of 52.48% male and 47.52% female, which is more balanced than MIMIC-III (56.15% male and 43.85% female).

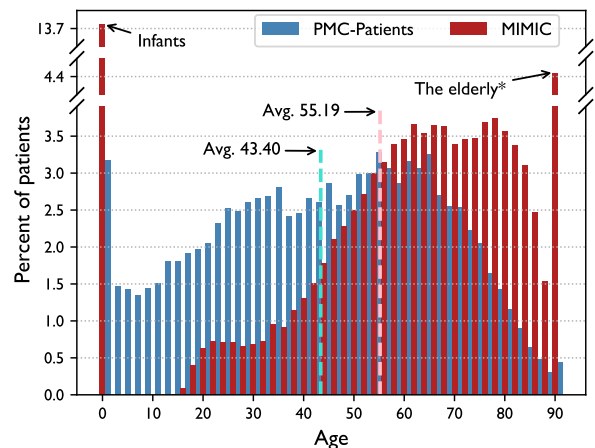


Figure 4: Patient age distributions of PMC-Patients compared to MIMIC-III. \* Exact ages of patients elder than 89 years old are obscured in MIMIC-III.

**Conditions** We also analyze the medical conditions associated with the patients: for PMC-Patients, we use the MeSH Diseases terms of the articles as a proxy; for MIMIC, we use the ICD codes. The most frequent medical conditions are shown in Figure 5. In PMC-Patients, the majority

Dataset	Count				Average Length / Note	
	Articles	Patients	Admissions	Notes	Sentences	Words
PMC-Patients	140,897	167,034	–	167,034	23.35	410.28
MIMIC-III (all)	–	46,146	58,362	2,022,302	19.09	222.51
MIMIC-III (d.s.)	–	41,127	52,726	59,568	108.11	1282.35

Table 2: Dataset statistics of PMC-Patients and MIMIC-III (contents in de-identification masks are not counted). d.s.: discharge summaries.

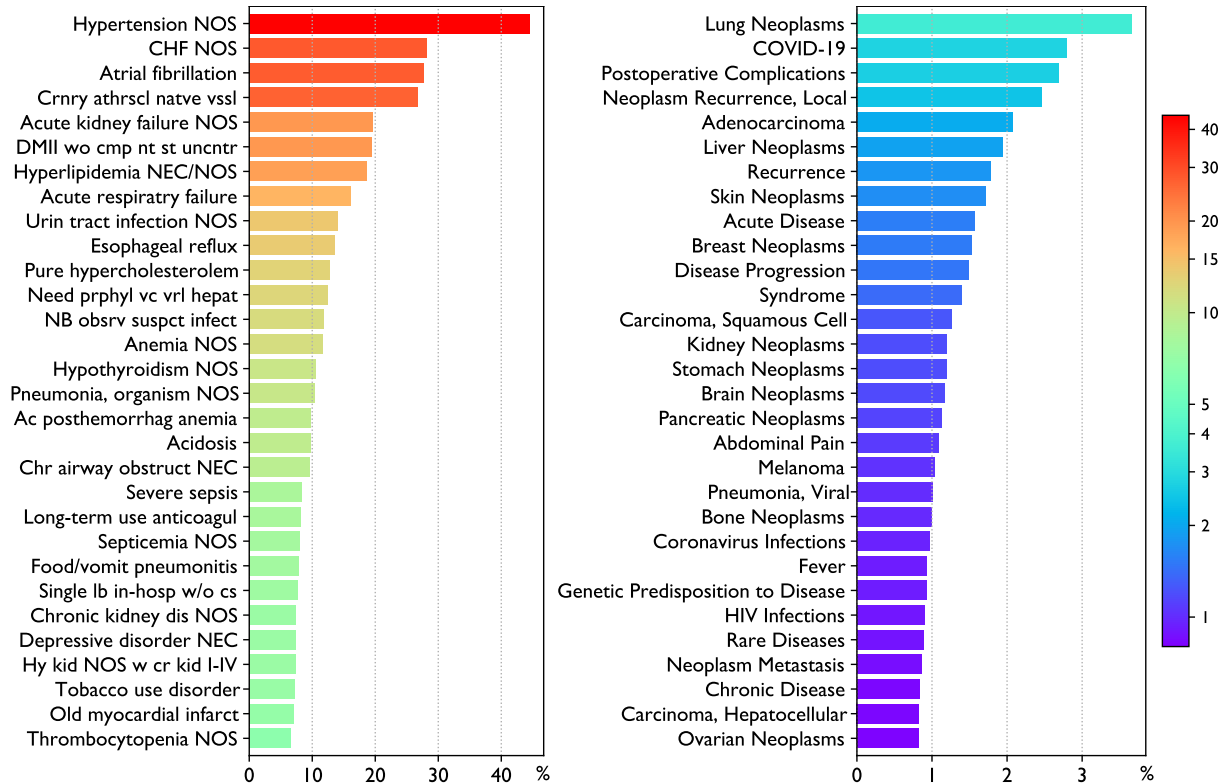


Figure 5: Frequency of top 30 ICD codes in MIMIC (left) and MeSH Diseases terms in PMC-Patients (right).

(16/30) of frequent conditions are related to cancer, with an interesting exception of COVID-19 as the second most frequent condition. In MIMIC-III, severe non-cancer diseases (e.g. congestive heart failure) have the highest relative frequencies, and their absolute values are much higher than those of the most frequent conditions in PMC-Patients. For example, hypertension and lung neoplasms are the most frequent condition in MIMIC-III and PMC-Patients, respectively. Over 40% of MIMIC-III patients have hypertension, while less than 4% of patients in PMC-Patients have lung neoplasms. In addition, PMC-Patients covers 4031/4933 (81.7%) MeSH Diseases terms, which is relatively more than the 6770/14567 (46.5%) ICD codes.

### 3.3 Relation Analysis

In PMC-Patients, there are over **3M patient-article relevance annotations**, with an average of 18.64 articles per patient, bridging patient notes and PubMed publications, and nearly **300k patient-patient similarity annotations** at two different levels, with an average of 1.76 per patient.

Figure 6 shows the distributions of relevance and similarity annotations per patient. As expected, the distributions are quite long-tailed, highlighting the richness of annotations in PMC-Patients. 497 patients have over 100 relevance annotations, with a maximum value at 1364, and 129 patients have over 20 similarity annotations, with a maximum value at 79.

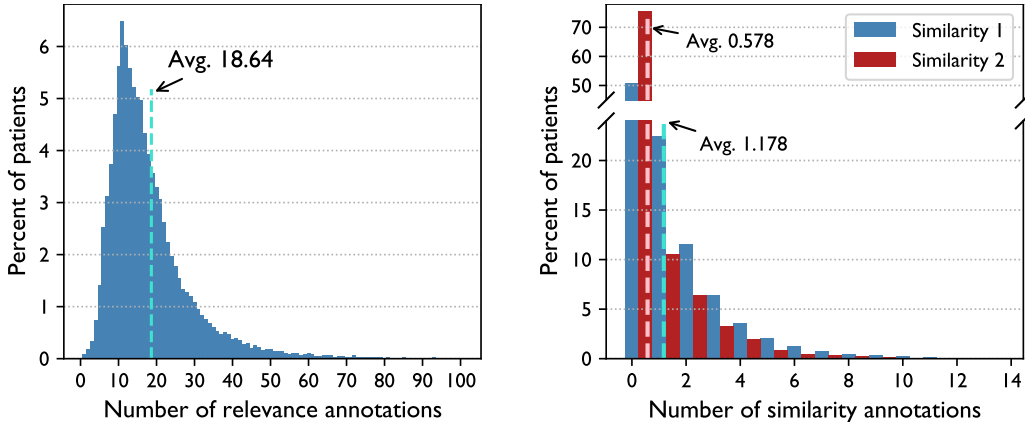


Figure 6: Distributions of relevance and similarity annotations (x-axis truncated).

## 4 Task 1: Patient Note Recognition

### 4.1 Objective

Though the patient notes in PMC-Patients are relatively clean (shown in Section 2.3), a large number of other potential patient notes in PMC are missed since the extraction triggers and the filters (especially `demographic_filter`) are quite strict. The goal of the Patient Note Recognition (PNR) task is to identify patient notes in the rest of PMC, where patient notes cannot be easily extracted by heuristics, and include such notes in PMC-Patients to form a “PMC-Patients-Large” dataset. Heuristically extracted patient notes in PMC-Patients can be used to train the PNR models.

### 4.2 Task Settings

We model PNR as a paragraph-level sequential labeling task, similar to the named entity recognition (NER) task. For each article, given input as a sequence of texts  $p_1, p_2, \dots, p_n$ , where  $n$  is the number of paragraphs, the output is a sequence of BIO tags  $t_1, t_2, \dots, t_n$ . Annotations are generated automatically during extraction. We randomly sample 5k articles as dev set and another 5k as test set. Notes extracted from articles in each split are denoted as **PMC-Patients-train/dev/test**, respectively. Table 3 shows the dataset statistics.

PNR performance is evaluated at two levels: **Note level**: Similar to NER F1 score, only valid predicted spans are taken as predicted notes, and predictions matching a ground truth note exactly are considered correct. Precision, recall, and F1 score are reported. **Paragraph level**: For each article, **precision** is defined by matching each predicted span with every true span, taking the maximum percentage of overlapped paragraphs (divided

by length of the predicted span), and taking the average of all predilections. **Recall** is defined in reverse, by matching each true span with predicted spans, dividing maximum overlap by length of the true span, and taking the average of all true spans. F1 is calculated using precision and recall defined above and taken average over articles.

Split	# Article	# Note	N. / A.
train	130,897	155,151	1.19
dev	5,000	5,924	1.19
test	5,000	5,959	1.19
human*	500	604	1.21
total	140,897	167,034	1.19

Table 3: Statistics of PNR dataset. N. / A.: average notes per article. \*Human evaluation set is a subset of test set and does not contribute to total counts.

### 4.3 Baseline Models

**Demographic Finder** We identify the beginning of a note with `demographic_filter` in Section 2.2 and tag the corresponding paragraph as "B". Other paragraphs are all labeled as "O".

**BERT** We fine-tune a BioBERT (Lee et al., 2020) and a Clinical BERT (Huang et al., 2019) classifier that tags each paragraph separately, without taking contexts of other paragraphs into consideration.

**CNN-LSTM-CRF** We use TextCNN (Zhang and Wallace, 2015) as the feature extractor for paragraphs and utilize BI-LSTM-CRF (Huang et al., 2015) model to perform sequential labeling.

Method / Annotation	Note Level			Paragraph Level		
	Precision	Recall	F1	Precision	Recall	F1
Demographic Finder	25.70	27.23	26.44	95.97	43.11	52.25
Clinical BERT (Huang et al., 2019)	87.81	89.11	88.45	97.41	95.13	94.15
BioBERT (Lee et al., 2020)	<b>89.09</b>	<b>90.26</b>	<b>89.67</b>	97.34	95.88	94.85
CNN-LSTM-CRF (Huang et al., 2015)	88.34	88.78	88.56	<b>97.39</b>	<b>96.47</b>	<b>95.36</b>
PMC-Patients	91.39	91.09	91.24	97.02	98.10	96.28
Expert A	97.99	96.70	97.34	99.02	98.89	98.11
Expert B	97.20	97.36	97.28	99.32	99.75	99.29

Table 4: PNR performance of different methods/annotations measured by final expert annotations (in percentages).

#### 4.4 Results

We use the final expert annotations (500 articles) in Section 2.3 as ground truths to evaluate PNR performances of different baseline models and annotations. The results are reported in Table 4.

Automated extraction of PMC-Patients presents high quality with a note-level F1 greater than 90% and is comparable to human expert performances in terms of paragraph-level metrics.

BioBERT achieves nearly 90% note-level F1 and CNN-LSTM-CRF’s paragraph-level F1 is just slightly lower than annotations, illustrating the possibility, empowered by PMC-Patients, of collecting a “PMC-Patients-Large” with high quality.

### 5 Task 2: Patient-Patient Similarity

#### 5.1 Objective

The goal of the patient-patient similarity (PPS) task is to measure similarity between any given pair of patients, which is the core task of patient-patient retrieval (PPR). Models pre-trained on PPS dataset can serve as a reranker for PPR task in Section 6.

#### 5.2 Task Settings

We model PPS as a 3-way classification task: each instance consists of a pair of notes  $n_0, n_1$  and a label  $l \in \{0, 1, 2\}$ . Labels 1 and 2 represent respective similarities (positive samples) and label 0 is given to randomly sampled irrelevant notes (negative samples). The ratio of positive to negative samples is 1:1.

For training set, both notes are collected from PMC-Patients-train while for dev/test set, one note is from PMC-Patients-dev/test and the other from the union of PMC-Patients-train and PMC-Patients-dev/test. Dataset statistics are reported in Table 5. Performance is evaluated by accuracy.

Split	# Inst.	# Sim-1	# Sim-2	# Neg.
train	257.4k	83.9k	44.8k	128.7k
dev	16.4k	6.5k	1.7k	8.2k
test	19.0k	7.7k	1.8k	9.5k
total	292.7k	98.1k	48.3k	146.4k

Table 5: Statistics of PPS dataset. Inst.: instances. Sim-1/2: similarity 1/2. Neg.: negative samples.

#### 5.3 Baseline Models

**Logistic Regression** For each pair of patient notes, we extract the following features to run a logistic regression (Berkson, 1944): 1. age difference:  $|a_1 - a_2|$ , where  $a_1$  and  $a_2$  are ages of the patients; 2. gender difference:  $I(g_1 = g_2)$ , where  $I$  denotes the indicator function and  $g_1, g_2$  are genders of the patients; 3. topic similarity:  $DSC(\mathcal{E}_1, \mathcal{E}_2)$ , where DSC denotes the Dice similarity coefficient (Dice, 1945) and  $\mathcal{E}_1, \mathcal{E}_2$  are sets of named entities detected by Scispacy (Neumann et al., 2019) in each note.

**BERT** We fine-tune a BioBERT and a Clinical BERT classifier that takes two notes separated by “[SEP]” token as input and outputs the probabilities of three labels.

#### 5.4 Results

Results on test set are reported in Table 6. Logistic regression, even using only topic similarity as a single feature, presents quite good performances, indicating that patients annotated as similar generally share similar topics, with more co-mentioned named entities. Besides, the ability of such a model to distinguish positive and negative samples by topic similarity verifies the diversity of topics in PMC-Patients.

Method	Acc (%)
Logistic Regression (DCS only)	79.06
Logistic Regression (all features)	79.52
Clinical BERT (Huang et al., 2019)	89.07
BioBERT (Lee et al., 2020)	<b>89.71</b>

Table 6: PPS performance of different methods.

BERT outperforms logistic regression by a large margin, and BioBERT outperforms Clinical BERT slightly. The confusion matrix shown in Figure 7 demonstrates the model’s capacity of distinguishing between different levels of similarity, and the most frequent mistakes are labeling pairs with similarity 1 as irrelevant.

It should be noted that many notes in PMC-Patients have token counts far exceeding BERT’s 512 token limits and truncation is applied in our baselines, which suffers from inevitable information loss. Efficient transformers (Tay et al., 2020), represented by Big bird (Zaheer et al., 2020) and Longformer (Beltagy et al., 2020), are potential solutions, and we leave that for future work.

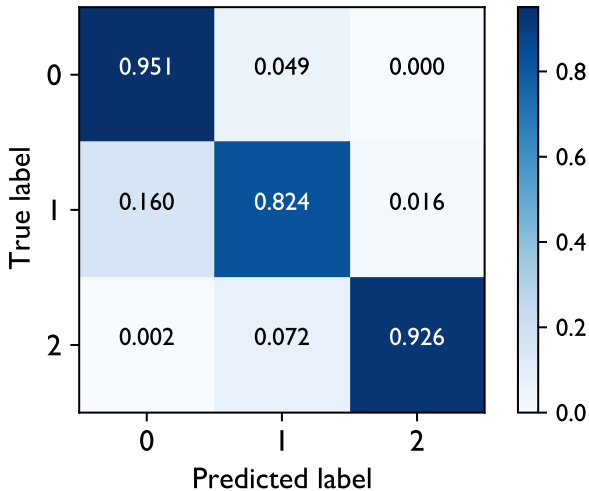


Figure 7: Confusion matrix given by BioBERT on PPS.

## 6 Task 3: Patient-Patient Retrieval

### 6.1 Objective

The goal of the Patient-Patient Retrieval (PPR) task is to retrieve similar patient notes in a large database (e.g.: a local EHR database or PMC-Patients) to any given patient note. The diagnosis, treatment responses, and prognosis of similar patients can provide evidence-based decision support for the given patient.

### 6.2 Task Settings

We model PPR as a 2-grade retrieval task, without distinguishing between two levels of similarity. Each patient note serves as a query and other notes constitute document collection  $\mathcal{D}$ . Note that some notes in PMC-Patients don’t have similarity annotations and are excluded from the queries.

For each split, queries are collected from the corresponding split of PMC-Patients. Documents of the training set only consist of PMC-Patients-train while dev/test set uses the union of PMC-Patients-dev/test and PMC-Patients-train as document collection. Dataset statistics are reported in Table 7.

PPR performance is evaluated with mean reciprocal rank (MRR), precision at 10 (P@10), and recall at 1k and 10k (R@1k, R@10k).

Split	# Q.	$ \mathcal{D} $	# Sim.	Sim. / Q.
train	94.6k	155.2k	257.4k	2.72
dev	3.7k	161.1k	10.0k	2.74
test	3.7k	161.1k	11.5k	3.10

Table 7: Statistics of PPR dataset. Q.: queries.  $\mathcal{D}$ : document collection. Sim.: similarity annotations.

### 6.3 Baseline Retrievers

**BM25** BM25 algorithm (Robertson et al., 1995) is a commonly used method for text retrieval, measuring similarity with term frequencies. We implement BM25 with Elasticsearch<sup>6</sup>, a widely used and highly efficient search engine.

**Embedding-Based Retrieval (EBR)** We feed each patient note into BioBERT and use the CLS embedding as the patient note embedding. Then Faiss (Johnson et al., 2017), a library for efficient similarity search and clustering of dense vectors, is utilized to search for similar notes by embedding.

**DSC** We use topic similarity defined in Section 5 as patient similarity score and rank all the patients.

### 6.4 Results

Table 8 shows that BM25 is a strong baseline with recall@10k over 90% and nearly 50% MRR, outperforming EBR by a large margin. The failure of EBR may be attributed to the inadequacy of using BERT to distinguish between notes without further fine-tuning. 10k randomly sampled notes present an average pairwise cosine similarity as

<sup>6</sup><https://www.elastic.co/elasticsearch/>



high as 0.95, illustrating that BERT tends to vastly overestimate similarities between notes.

Method	MRR	P@10	R@1k	R@10k
EBR	7.92	1.42	13.50	27.70
DSC	45.05	10.05	68.83	86.93
BM25	<b>48.83</b>	<b>11.23</b>	<b>77.77</b>	<b>91.84</b>

Table 8: PPR performance of different retrievers (in percentages).

## 7 Task 4: Patient-Article Retrieval

### 7.1 Objective

The goal of the Patient-Article Retrieval (PAR) is to find relevant scientific articles in PubMed to any given patient note. Such articles can provide clinical decision supports for the management of the given patient.

### 7.2 Task Settings

We model PAR as a 2-grade retrieval task where each patient note serves as a query and document collection  $\mathcal{D}$  consists of titles and abstracts of all PubMed publications with machine-readable titles or abstracts. Dataset split is based on patient notes (queries) split. Dataset statistics are reported in Table 9.

Split	# Q.	$ \mathcal{D} $	# Rel.	Rel. / Q.
train	155.2k	33.5M	2.9M	18.64
dev	5.9k	33.5M	107.5k	18.14
test	6.0k	33.5M	114.1k	19.14

Table 9: Statistics of PAR dataset. Q.: queries.  $\mathcal{D}$ : document collection. Rel.: relevance annotations.

### 7.3 Baseline Retrievers

**BM25** Similar to PPR task, we present BM25 implemented with Elasticsearch as a baseline.

**KNN** For each query patient in test set, we first retrieve similar patients (nearest neighbors) in only PMC-Patients-train using BM25, then take their relevance annotations (training set of PAR) as candidates. Note that there are articles relevant to multiple patients, so the relevance score between an article and the query is defined as the sum of similarity scores of all retrieved relevant patients.

## 7.4 Results

BM25 performs much worse on PAR than PPR, as shown in Table 8 and Table 10, indicating that compared to PPR, PAR is much more challenging. The potential reasons lie in the much larger document collection in PAR and differences between patient notes and article abstracts. KNN gives better results but the metrics are still quite low, leaving much room for improvement.

Method	MRR	P@10	R@1k	R@10k
BM25	14.37	3.69	16.95	32.31
KNN	<b>18.62</b>	<b>5.86</b>	<b>26.36</b>	<b>42.93</b>

Table 10: PAR performance of different retrievers (in percentages).

## 8 Related Works

PMC-Patients is basically a case report dataset that: 1. contains patient notes similar to clinical narratives and 2. is annotated with patient-patient similarity and patient-article relevance information. In this section, we discuss four categories of related works: case report datasets, clinical narrative datasets, patient-patient retrieval datasets, and patient-article retrieval datasets.

### 8.1 Case Report Datasets

Case report datasets are typically extracted from published articles (case reports). [Caufield et al. \(2018\)](#) develop a reference set of 3,100 curated clinical case reports with standardized metadata template. CAS is a corpus that contains 4,900 clinical cases in French ([Grabar et al., 2020](#); [Grouin et al., 2019](#)), which are collected from journals and websites in French-speaking countries. [Smalheiser et al. \(2019\)](#) introduce a dataset of 500 case reports annotated with main finding sentences. [Schulz et al. \(2020\)](#) release a corpus consisting of 53 case report documents annotated with medical entities and entity relations. The E3C project ([Magnini et al., 2021](#)) collects a multilingual corpus of about 32k documents covering 5 European languages, with a small proportion temporally annotated. PharmaCoNER ([Gonzalez-Agirre et al., 2019](#)) is a corpus of 1,000 clinical case studies manually annotated with pharmacological entities. The BARR2 corpus ([Intxaurreondo et al., 2018](#)) contains 684 Spanish case reports annotated with abbreviations and their definitions. CliCR ([Šuster and Daelemans, 2018](#))

reformulates about 12k case reports to 100k gap-filling machine reading comprehension instances.

Compared to these works, PMC-Patients is much larger, in English, and contains document-level relevance annotations.

## 8.2 Clinical Narrative Datasets

Apart from MIMIC that has already been discussed and compared above, several other clinical narrative datasets have also been proposed, which are mostly collected from EHRs. MTSamples<sup>7</sup> contains 5k sample transcription reports. The THYME project (Styler et al., 2014), which is aimed at extracting useful temporal relations from clinical narratives, has released a corpus of about 1.2k clinical, pathology, and radiology records for patients with brain and colon cancer. The n2c2<sup>8</sup> (originally named i2b2<sup>9</sup>) project has released many clinical note datasets that are specifically annotated with certain information, e.g. de-identification (Uzuner et al., 2007), obesity status (Uzuner, 2009), concept relations (Uzuner et al., 2011) and cohort selection (Stubbs et al., 2019). The OHNLP Challenges (Wang et al., 2018, 2020) release about 2k sentence pairs in EHR notes with similarity annotations. MedNLI (Romanov and Shivade, 2018) annotates 14k sentence pairs from MIMIC for clinical language inference. These datasets are manually annotated and thus limited by size, typically containing several hundred to a few thousand clinical note pieces which only reflect part of patients’ medical situations.

Grabar et al. (2020) show that case reports and clinical narratives have high textual similarity, so PMC-Patients has the potential to facilitate the processing and understanding of clinical narratives.

## 8.3 Patient-Patient Retrieval Datasets

To build a patient-patient retrieval dataset, it is essential to define and calculate patient-patient similarity, which is a hard research question (Seligson et al., 2020) and there are many ongoing efforts (Sharafoddini et al., 2017; Parimbelli et al., 2018). However, to the best of our knowledge, no publicly available similar patient retrieval dataset exists, possibly due to the difficulty of defining patient similarity. There are only a few works on similar patient retrieval (Plaza and Díaz, 2010; Arnold

et al., 2010), all of which use private datasets and annotations.

In PMC-Patients, we leave the hard task of patient-patient similarity definition to case report authors, who usually cite other case reports that contain similar patients and describe their similarity in the corresponding anchor texts.

## 8.4 Patient-Article Retrieval Datasets

The Text REtrieval Conference (TREC) has organized several challenges on retrieving relevant documents for given patient queries: The Clinical Decision Support (CDS, 2014-2016) tracks focus on retrieving relevant PMC articles for given patient summary notes with specific intents (e.g.: finding treatment/diagnosis) (Simpson et al., 2014; Roberts et al., 2015, 2016); The Precision Medicine (PM, 2017-2020) tracks focus on retrieving relevant PubMed articles and eligible clinical trials for given semi-structured patient queries, which include demographics, cancer types, gene mutations, and tentative treatments (Roberts et al., 2017, 2018, 2019, 2020); The Clinical Trial (CT, 2021) track<sup>10</sup> focuses on retrieving eligible clinical trials for given patient summary notes.

Each year, 30-75 patient queries (topics) will be released and about 30k submitted patient-document pairs will be annotated with relevance for evaluation. Annotations of previous years are usually used to train next years’ participating systems. Though the annotation size is relatively large, the diversity of patient queries is severely limited. PMC-Patients provides over 3M relevant article annotations of 167k patients, where relevance is also defined by the case report authors.

## 9 Conclusions and Future Works

In this paper, we present PMC-Patients, a publicly available, large-scale, high-quality, and diverse patient note dataset that is annotated with patient-patient similarity and patient-article relevance labels. PMC-Patients can be used to find more patient notes, calculate patient-patient similarity, and retrieve similar patients or relevant articles for any given patient note.

PMC-Patients will be updated in the future from the following perspectives: 1. collecting a “PMC-Patients-Large” with distant supervision; 2. incorporating human evaluations of PPR and PAR

<sup>7</sup>[www.mtsamples.com](http://www.mtsamples.com)

<sup>8</sup><https://n2c2.dbmi.hms.harvard.edu/>

<sup>9</sup><https://www.i2b2.org/NLP/DataSets/Main.php>

<sup>10</sup><http://www.trec-cds.org/2021.html>

datasets; and 3. leveraging diverse information including tables, figures, and journal attributes. There is also much room for improving downstream tasks' performances. More elaborate sampling methods in PPS, such as ones that introduce multi-hop citations (connected by intermediate articles, rather than directly cited), and corresponding graph-based encoding methods may help rerank candidates and generate better results in PPR. Besides, more sophisticated rerankers, especially ones able to process long texts, can be designed to improve performances in PPR and PAR tasks.

## References

- Emily Alsentzer, John Murphy, William Boag, Weihung Weng, Di Jindi, Tristan Naumann, and Matthew McDermott. 2019. Publicly available clinical bert embeddings. In *Proceedings of the 2nd Clinical Natural Language Processing Workshop*, pages 72–78.
- Corey W Arnold, Suzie M El-Saden, Alex AT Bui, and Ricky Taira. 2010. Clinical case-based retrieval using latent topic analysis. In *AMIA annual symposium proceedings*, volume 2010, page 26. American Medical Informatics Association.
- Iz Beltagy, Matthew E Peters, and Arman Cohan. 2020. Longformer: The long-document transformer. *arXiv preprint arXiv:2004.05150*.
- Joseph Berkson. 1944. Application of the logistic function to bio-assay. *Journal of the American statistical association*, 39(227):357–365.
- Tom B Brown, Benjamin Mann, Nick Ryder, Melanie Subbiah, Jared Kaplan, Prafulla Dhariwal, Arvind Neelakantan, Pranav Shyam, Girish Sastry, Amanda Askell, et al. 2020. Language models are few-shot learners. *arXiv preprint arXiv:2005.14165*.
- J Harry Caufield, Yijiang Zhou, Anders O Garlid, Shaun P Setty, David A Liem, Quan Cao, Jessica M Lee, Sanjana Murali, Sarah Spendlove, Wei Wang, et al. 2018. A reference set of curated biomedical data and metadata from clinical case reports. *Scientific data*, 5(1):1–18.
- Wendy W Chapman, Prakash M Nadkarni, Lynette Hirschman, Leonard W D'Avolio, Guergana K Savova, and Ozlem Uzuner. 2011. Overcoming barriers to nlp for clinical text: the role of shared tasks and the need for additional creative solutions.
- Jacob Devlin, Ming-Wei Chang, Kenton Lee, and Kristina Toutanova. 2019. **BERT: Pre-training of deep bidirectional transformers for language understanding**. In *Proceedings of the 2019 Conference of the North American Chapter of the Association for Computational Linguistics: Human Language Technologies, Volume 1 (Long and Short Papers)*, pages 4171–4186, Minneapolis, Minnesota. Association for Computational Linguistics.
- Lee R Dice. 1945. Measures of the amount of ecologic association between species. *Ecology*, 26(3):297–302.
- Amit X Garg, Neill KJ Adhikari, Heather McDonald, M Patricia Rosas-Arellano, Philip J Devereaux, Joseph Beyene, Justina Sam, and R Brian Haynes. 2005. Effects of computerized clinical decision support systems on practitioner performance and patient outcomes: a systematic review. *JAMA*, 293(10):1223–1238.
- Aitor Gonzalez-Agirre, Montserrat Marimon, Ander Intxaurrenondo, Obdulia Rabal, Marta Villegas, and Martin Krallinger. 2019. Pharmaconer: Pharmacological substances, compounds and proteins named entity recognition track. In *Proceedings of The 5th Workshop on BioNLP Open Shared Tasks*, pages 1–10.
- Natalia Grabar, Clément Dalloux, and Vincent Claveau. 2020. Cas: corpus of clinical cases in french. *Journal of Biomedical Semantics*, 11(1):1–10.
- Cyril Grouin, Natalia Grabar, Vincent Claveau, and Thierry Hamon. 2019. Clinical case reports for nlp. In *BioNLP 2019-18th ACL Workshop on Biomedical Natural Language Processing*, pages 273–282. ACL.
- Kexin Huang, Jaan Altosaar, and Rajesh Ranganath. 2019. Clinicalbert: Modeling clinical notes and predicting hospital readmission. *arXiv preprint arXiv:1904.05342*.
- Zhiheng Huang, Wei Xu, and Kai Yu. 2015. Bidirectional lstm-crf models for sequence tagging. *arXiv preprint arXiv:1508.01991*.
- Ander Intxaurrenondo, Montserrat Marimón, Aitor González-Agirre, Jose Antonio Lopez-Martin, Heidy Rodriguez, Jesus Santamaria, Marta Villegas, and Martin Krallinger. 2018. Finding mentions of abbreviations and their definitions in spanish clinical cases: The barr2 shared task evaluation results. *IberEval@ SEPLN*, 2150:280–289.
- Alistair EW Johnson, Tom J Pollard, Lu Shen, H Lehman Li-Wei, Mengling Feng, Mohammad Ghassemi, Benjamin Moody, Peter Szolovits, Leo Anthony Celi, and Roger G Mark. 2016. MIMIC-III, a freely accessible critical care database. *Scientific data*, 3(1):1–9.
- Jeff Johnson, Matthijs Douze, and Hervé Jégou. 2017. Billion-scale similarity search with gpus. *arXiv preprint arXiv:1702.08734*.
- Amir Karami, Mehdi Ghasemi, Souvik Sen, Marcos F Moraes, and Vishal Shah. 2019. Exploring diseases and syndromes in neurology case reports from 1955 to 2017 with text mining. *Computers in biology and medicine*, 109:322–332.

- Kensaku Kawamoto, Caitlin A Houlihan, E Andrew Balas, and David F Lobach. 2005. Improving clinical practice using clinical decision support systems: a systematic review of trials to identify features critical to success. *BMJ*, 330(7494):765.
- Matthieu Komorowski, Leo A Celi, Omar Badawi, Anthony C Gordon, and A Aldo Faisal. 2018. The artificial intelligence clinician learns optimal treatment strategies for sepsis in intensive care. *Nature medicine*, 24(11):1716–1720.
- Angelina Prima Kurniati, Eric Rojas, David Hogg, Geoff Hall, and Owen A Johnson. 2019. The assessment of data quality issues for process mining in healthcare using medical information mart for intensive care iii, a freely available e-health record database. *Health informatics journal*, 25(4):1878–1893.
- Jinhyuk Lee, Wonjin Yoon, Sungdong Kim, Donghyeon Kim, Sunkyu Kim, Chan Ho So, and Jaewoo Kang. 2020. Biobert: a pre-trained biomedical language representation model for biomedical text mining. *Bioinformatics*, 36(4):1234–1240.
- Bernardo Magnini, Begona Altuna, Alberto Lavelli, Manuela Speranza, and Roberto Zanoli. 2021. The e3c project: European clinical case corpus. *Language*, 1(L2):L3.
- James Mullenbach, Sarah Wiegrefe, Jon Duke, Jimeng Sun, and Jacob Eisenstein. 2018. Explainable prediction of medical codes from clinical text. In *Proceedings of the 2018 Conference of the North American Chapter of the Association for Computational Linguistics: Human Language Technologies, Volume 1 (Long Papers)*, pages 1101–1111.
- Mark Neumann, Daniel King, Iz Beltagy, and Waleed Ammar. 2019. *ScispaCy: Fast and Robust Models for Biomedical Natural Language Processing*. In *Proceedings of the 18th BioNLP Workshop and Shared Task*, pages 319–327, Florence, Italy. Association for Computational Linguistics.
- Enea Parimbelli, Simone Marini, Lucia Sacchi, and Riccardo Bellazzi. 2018. Patient similarity for precision medicine: A systematic review. *Journal of biomedical informatics*, 83:87–96.
- Laura Plaza and Alberto Díaz. 2010. Retrieval of similar electronic health records using umls concept graphs. In *International Conference on Application of Natural Language to Information Systems*, pages 296–303. Springer.
- Kirk Roberts, Dina Demner-Fushman, Ellen M Voorhees, Steven Bedrick, and William R Hersh. 2020. Overview of the trec 2020 precision medicine track. In *The Twenty-Ninth Text REtrieval Conference (TREC) Proceedings*.
- Kirk Roberts, Dina Demner-Fushman, Ellen M Voorhees, and William R Hersh. 2016. Overview of the trec 2016 clinical decision support track. In *The Twenty-fifth Text REtrieval Conference (TREC) Proceedings*.
- Kirk Roberts, Dina Demner-Fushman, Ellen M Voorhees, William R Hersh, Steven Bedrick, and Alexander J Lazar. 2018. Overview of the trec 2018 precision medicine track. In *The Twenty-Seventh Text REtrieval Conference (TREC) Proceedings*.
- Kirk Roberts, Dina Demner-Fushman, Ellen M Voorhees, William R Hersh, Steven Bedrick, Alexander J Lazar, and Shubham Pant. 2017. Overview of the trec 2017 precision medicine track. In *The Twenty-Sixth Text REtrieval Conference (TREC) Proceedings*, volume 26.
- Kirk Roberts, Dina Demner-Fushman, Ellen M Voorhees, William R Hersh, Steven Bedrick, Alexander J Lazar, Shubham Pant, and Funda Meric-Bernstam. 2019. Overview of the trec 2019 precision medicine track. In *The Twenty-Eighth Text REtrieval Conference (TREC) Proceedings*.
- Kirk Roberts, Matthew S Simpson, Ellen M Voorhees, and William R Hersh. 2015. Overview of the trec 2015 clinical decision support track. In *The Twenty-fourth Text REtrieval Conference (TREC) Proceedings*.
- Stephen E Robertson, Steve Walker, Susan Jones, Micheline M Hancock-Beaulieu, Mike Gatford, et al. 1995. Okapi at trec-3. *Nist Special Publication Sp*, 109:109.
- Alexey Romanov and Chaitanya Shivade. 2018. Lessons from natural language inference in the clinical domain. In *Proceedings of the 2018 Conference on Empirical Methods in Natural Language Processing*, pages 1586–1596.
- Sarah Schulz, Jurica Ševa, Samuel Rodriguez, Malte Ostendorff, and Georg Rehm. 2020. Named entities in medical case reports: Corpus and experiments. *arXiv preprint arXiv:2003.13032*.
- Nathan D Seligson, Jeremy L Warner, William S Dalton, David Martin, Robert S Miller, Debra Patt, Kenneth L Kehl, Matvey B Palchuk, Gil Alterovitz, Laura K Wiley, et al. 2020. Recommendations for patient similarity classes: results of the amia 2019 workshop on defining patient similarity. *Journal of the American Medical Informatics Association*, 27(11):1808–1812.
- Anis Sharafoddini, Joel A Dubin, Joon Lee, et al. 2017. Patient similarity in prediction models based on health data: a scoping review. *JMIR medical informatics*, 5(1):e6730.
- Matthew S Simpson, Ellen M Voorhees, and William Hersh. 2014. Overview of the trec 2014 clinical decision support track. Technical report.
- Neil R Smalheiser, Mengqi Luo, Sidharth Addepalli, and Xiaokai Cui. 2019. A manual corpus of annotated main findings of clinical case reports. *Database*, 2019.

Amber Stubbs, Michele Filannino, Ergin Soysal, Samuel Henry, and Özlem Uzuner. 2019. Cohort selection for clinical trials: n2c2 2018 shared task track 1. *Journal of the American Medical Informatics Association*, 26(11):1163–1171.

William F Styler, Steven Bethard, Sean Finan, Martha Palmer, Sameer Pradhan, Piet C De Groen, Brad Erickson, Timothy Miller, Chen Lin, Guergana Savova, et al. 2014. Temporal annotation in the clinical domain. *Transactions of the association for computational linguistics*, 2:143–154.

Simon Šuster and Walter Daelemans. 2018. Clicr: A dataset of clinical case reports for machine reading comprehension. *arXiv preprint arXiv:1803.09720*.

Yi Tay, Mostafa Dehghani, Dara Bahri, and Donald Metzler. 2020. Efficient transformers: A survey. *arXiv preprint arXiv:2009.06732*.

Özlem Uzuner. 2009. Recognizing obesity and comorbidities in sparse data. *Journal of the American Medical Informatics Association*, 16(4):561–570.

Özlem Uzuner, Yuan Luo, and Peter Szolovits. 2007. Evaluating the state-of-the-art in automatic identification. *Journal of the American Medical Informatics Association*, 14(5):550–563.

Özlem Uzuner, Brett R South, Shuying Shen, and Scott L DuVall. 2011. 2010 i2b2/va challenge on concepts, assertions, and relations in clinical text. *Journal of the American Medical Informatics Association*, 18(5):552–556.

Yanshan Wang, Naveed Afzal, Sijia Liu, Majid Rastegar-Mojarad, Liwei Wang, Feichen Shen, Sunyang Fu, and Hongfang Liu. 2018. Overview of the biocreative/ohnlp challenge 2018 task 2: clinical semantic textual similarity. *Proceedings of the BioCreative/OHNL Challenge*, 2018.

Yanshan Wang, Sunyang Fu, Feichen Shen, Sam Henry, Ozlem Uzuner, Hongfang Liu, et al. 2020. The 2019 n2c2/ohnlp track on clinical semantic textual similarity: overview. *JMIR Medical Informatics*, 8(11):e23375.

Stephen Wu, Kirk Roberts, Surabhi Datta, Jingcheng Du, Zongcheng Ji, Yuqi Si, Sarvesh Soni, Qiong Wang, Qiang Wei, Yang Xiang, et al. 2020. Deep learning in clinical natural language processing: a methodical review. *Journal of the American Medical Informatics Association*, 27(3):457–470.

Manzil Zaheer, Guru Guruganesh, Kumar Avinava Dubey, Joshua Ainslie, Chris Alberti, Santiago Ontanon, Philip Pham, Anirudh Ravula, Qifan Wang, Li Yang, et al. 2020. Big bird: Transformers for longer sequences. *Advances in Neural Information Processing Systems*, 33:17283–17297.

Ye Zhang and Byron Wallace. 2015. A sensitivity analysis of (and practitioners’ guide to) convolutional neural networks for sentence classification. *arXiv preprint arXiv:1510.03820*.

## A Samples of PMC-Patients

Table 11 gives several samples of PMC-Patients. To give examples of the relational annotations, we sample two anchor patients and then take samples from their annotations randomly.

Table 11: Samples of PMC-Patients. Id: patient\_uid for note and pubmed\_id for pubmed article. Text: patient note or pubmed title (in bold) and abstract. Annotations: similarity annotations are given by patient\_uid and relevance annotations are given by pubmed\_id. Annotations in red are presented in this table.

Id	Text	Annotations
patient_uid 8718394-1	<p>A 53-year-old woman was referred to our clinic with waist and back pain and numbness of the lower limbs for more than 1 month. The pain was not related to her posture and became more prominent when she moved. She had a medical history of lumbar disc herniation and no history of trauma. On initial evaluation, her vital signs were stable. Apart from the pain of the waist and back, physical examination revealed unremarkable findings. Routine blood tests were obtained. Further, liver function tests revealed normal results. The blood CA199, CA125, CEA, and AFP levels were also within normal limits. Computed tomography of the chest revealed scattered pulmonary nodules with calcifications associated with a soft tissue mass measuring 3.3 cm × 2.4 cm and without pleural thickening at the superior lobe of the right lung (SOMATOM definition, Siemens Healthcare, Erlangen, Germany; tube voltage, 100-120 kVp; tube current, 450 mA; slice thickness, 0.625 mm; pitch, 0.992:1; rotation speed: 0.5 s/rot; ASIR-V:30%). Enlarged lymph nodes of the right hilar were also evident. Abdominal contrast-enhanced CT revealed diffuse lesions with massive calcifications in the liver, which shows faint peripheral enhancement in the arterial phase and low enhancement in the portal phase (Iopromide Injection, Bayer Pharma AG; the arterial phase and portal venous phase were obtained at 25 s and 60 s after contrast injection.). The largest lesion measuring 10.2 cm × 7.5 cm was located in the right lobe of the liver and ( ). CT examination also revealed osteolytic lesions with a massive thick sclerotic rim in the right second rib, 11th thoracic vertebra, and first lumbar spine. Bone scintigraphy with 99mTc-methylene diphosphonate showed multiple hypermetabolic activities in the involved bones ( ). Cerebral magnetic resonance imaging (MRI) revealed no anomalies. The patient underwent transthoracic needle biopsy of the largest pulmonary lesion located in the right superior lobe. Histopathological analysis revealed epithelioid cells arranged in a glandular pattern with clear cytoplasm ( ). Immunohistochemical staining showed that the neoplastic cells were positive for CD31, CD34, CAMTA1, and EMA, but negative for ERG, TFE3, PCK, and desmin, with a Ki-67 index rate of 10%. Histopathological examination indicated a rare low-grade malignant vascular neoplasm, confirming the diagnosis of EHE. Considering the multiple intra-pulmonary, right hilar lymph node, liver, and bone metastases, the patient was treated with chemotherapy with paclitaxel liposome (240 mg/m<sup>2</sup>; day 1) and carboplatin (550 mg/m<sup>2</sup>; day 1). At 8 months, the patient had completed four cycles of combination therapy. There were no changes in the patient's disease status on CT at the 8-month follow-up visit.</p>	<p><b>Similarity 1</b> 3678532-1, 3678532-2, 3678532-3. <b>Relevant</b> 1302463, 17019735, 24944653, 3522725, 26137035, 31209195, 25992243, 21546438, ...</p>
patient_uid 3678532-1	<p>The patient was a 40-year-old Asian male with a four-month history of a dry cough, dyspnea and hemoptysis. The patient was a heavy smoker with an unremarkable medical history. A chest computed tomography (CT) scan revealed the presence of multiple nodules scattered in both lungs without hilar and mediastinal lymphadenopathy or pleural effusion ( ). Initially, a bronchofibroscope examination failed to reveal any abnormalities. In order to obtain a definitive diagnosis, the tissue specimens were taken by diagnostic right thoracoscopic lung biopsy. The histological diagnosis of PEH was based on the pathological examination. The pathological examination of the biopsied specimen revealed that the center of the pulmonary nodule was sclerotic and hypocellular, with hyalinization and calcification. The tumor cells were round with abundant eosinophilic cytoplasm, intracytoplasmic vacuolization and a signet ring-like appearance ( ). Immunohistochemical analysis revealed that the tumor cells were positive for the endothelial markers, factor-VIII-related antigen and CD34 ( ). PEH disease progressed rapidly in this patient one month after pulmonary surgery. The T1-weighted magnetic resonance imaging (MRI) section examination revealed a nodular lesion in the brain, which was strongly suggestive of brain metastasis ( ). The CT revealed a spreading of the nodules throughout both lungs three months after surgery ( ). At this point, the patient began treatment with one cycle of chemotherapy with cisplatin, paclitaxel and endostar (15 mg/day for 14 consecutive days). The patient demonstrated improvements in dyspnea and a dramatic improvement in their clinical status. However, no change in the size of the pulmonary nodules over the period of chemotherapy was observed. The patient subsequently received another two cycles (two, bi-weekly) of chemotherapy treatment with carboplatin, paclitaxel and endostar. No significant reduction was observed in the tumor size and number, and the disease progressed. Following three months of stabilization, progression of the disease was evident. Therefore, the patient was discharged without further treatment. The patient survived for six months following the initial diagnosis.</p>	<p><b>Similarity 1</b> 7175060-1, 8718394-1, 7568163-1, ... <b>Similarity 2</b> 3678532-2, 3678532-3. <b>Relevant</b> 8996023, 7093931, ...</p>
patient_uid 3678532-2	<p>The patient was a 54-year-old female, non-smoker, who complained of chest pain, dyspnea and a dry cough for 11 months. A chest CT scan revealed intrapulmonary masses in the bilateral superior lobes, and a small right pleural effusion. Abdominal and pelvic CT scans did not reveal any lesions. A thoracoscopic lung biopsy from the right superior lobe was performed in order to examine the nodules. The postoperative course of the patient during follow-up was uneventful. Examination of the nodular sections revealed clusters of neoplastic cells as well as individual tumor cells. The normal pulmonary architecture was replaced by alveoli containing nodules of neoplastic cells and matrix. The histological features of pulmonary epithelioid hemangioendothelioma (EHE) were evident with confirmatory CD31 and CD34 immunohistochemical stains. No markers of mesothelial and muscular differentiation were observed. As a result, the patient was diagnosed with PEH. Immediately following confirmation of the diagnosis, combination chemotherapy with carboplatin, paclitaxel and bevacizumab (15 mg/kg) was initiated for six cycles, without distinct toxicities. The stabilization of the disease was evident, as the chest pain gradually subsided. Following eight months of stabilization, progression of the disease was evident. The patient survived for 15 months following the initial diagnosis.</p>	<p><b>Similarity 1</b> 8718394-1, ... <b>Similarity 2</b> 3678532-1, 3678532-3. <b>Relevant</b> 7093931, ...</p>
pubmed_id 24944653	<p><b>Hepatic epithelioid hemangioendothelioma: A comparison of Western and Chinese methods with respect to diagnosis, treatment and outcome</b></p> <p>Hepatic epithelioid hemangioendothelioma (HEHE) is a rare tumor of vascular origin. Whether HEHE in Chinese patients exhibits similar characteristics compared with Western patients is not well known. The aim of the present study was to summarize the characteristics of HEHE in Chinese patients and identify its prognostic factors. In total, six patients diagnosed with HEHE at the Beijing Friendship Hospital between 2000 and 2012 were combined with 44 previously reported cases in China, retrieved from the literature between 1989 and mid-2012. These 50 cases from China were compared with 402 patients from Western populations. Prognostic factors were identified by the test and Cox regression analysis. The male to female ratio of the Chinese patients was 1:2.1 with the mean age of 44.2 years (range, 22-86 years). The percentage of asymptomatic Chinese patients was significantly higher than in the Western patients (40.0 vs. 24.8%; P=0.026), and that of extrahepatic metastasis (16.0 vs. 36.6%; P=0.005) was significantly lower in Chinese patients. On imaging study, capsular retraction (59.5%) and calcification (26.0%), as well as positivity of CD34 (93.5%) and CD31 (80.6%), were more frequently found in the Chinese patients. Management for the Chinese patients included liver resection (LRx; 45.7%), liver transplantation (LTx; 5.7%), trans-catheter arterial chemoembolization (14.3%) and palliative treatment (34.3%). Chinese patients with larger-sized tumor nodules [relative risk (RR), 1.58; 95% confidence interval (CI), 1.032-2.422; P=0.035] and diffuse type (RR, 12.17; 95% CI, 1.595-92.979; P=0.016) exhibited unfavorable outcomes. In contrast to Western patients with HEHE, a larger number of Chinese patients were asymptomatic with less extrahepatic metastasis. In China, LRx is widely adopted rather than LTx. Chinese patients with large tumor size or diffuse type may encounter a poorer prognosis.</p>	<p>-</p>

Table 11: Samples of PMC-Patients. Id: patient\_uid for note and pubmed\_id for pubmed article. Text: patient note or pubmed title (in bold) and abstract. Annotations: similarity annotations are given by patient\_uid and relevance annotations are given by pubmed\_id. Annotations in red are presented in this table.

Id	Text	Annotations
pubmed_id 7093931	<p><b>Epithelioid hemangioendothelioma: a vascular tumor often mistaken for a carcinoma</b> Epithelioid hemangioendothelioma is a unique tumor of adult life which is characterized by an "epithelioid" or "histiocytoid" endothelial cell. Forty-one cases of this rare tumor have been recognized at the Armed Forces Institute of Pathology. They may occur in either superficial or deep soft tissue, and in 26 cases appeared to arise from a vessel, usually a medium-sized or large vein. They are composed of rounded or slightly spindled eosinophilic endothelial cells with rounded nuclei and prominent cytoplasmic vacuolization. The latter feature probably represents primitive lumen formation by a single cell. The cells grown in small nests or cords and only focally line well-formed vascular channels. The pattern of solid growth and the epithelioid appearance of the endothelium frequently leads to the mistaken diagnosis of metastatic carcinoma. The tumor can be distinguished from a carcinoma by the lack of pleomorphism and mitotic activity in most instances and by the presence of focal vascular channels. Ultrastructural study in four cases confirmed the endothelial nature of the tumor in demonstrating cells surrounded by basal lamina, dotted with surface pinocytotic vesicles, and occasionally containing Weibel-Palade bodies. Follow-up information in 31 cases indicated that 20 patients were alive and well following therapy; three developed local recurrences and six metastases. It is suggested the term epithelioid hemangioendothelioma be used to designate these biologically "borderline" neoplasms. The significance of the epithelioid endothelial cell is not entirely clear. Since it may be observed in both benign and malignant vascular lesions, its presence alone does not define a clinicopathologic entity.</p>	-
patient_uid 5901269-1	<p>A 60-year-old male presented to our outpatient clinic for a routine visit. He had no complaints except for minimal hand dryness and denied fatigue, generalized weakness, heat or cold intolerance, constipation, diarrhea, hair loss, or any recent weight changes. His past medical history was pertinent for a basal cell carcinoma of scalp treated with extensive excision 3 years prior. On physical examination, an enlarged, firm, non-tender thyroid gland was appreciated with about 3 cm left thyroid lobe mass felt on palpation. Xerosis of hands, arms, and legs were also noted with no pruritus or erythematous rash. No palpable lymphadenopathies or hepatosplenomegaly was noted. He denied any lump like sensation in his neck, neck pain, difficulty in swallowing, hoarseness, or dry cough. Signs of tracheal, esophageal, or neck vein compression were not found. He was an active smoker (35 pack-years) but did not have any history of radiation exposure, family history of thyroid-related disorders, or malignancy. His diet was normal with iodine-rich meals. Complete blood count and basic metabolic profile were within normal limits. TSH was found to be elevated at 10.14 uIU/mL. All other lab values were within normal limit. Thyroid ultrasound was done which revealed large 5.8 00d7 3.1 00d7 2.5 cm hypochoic mass occupying almost complete volume of the left thyroid lobe, and persistent elevation of TSH was found in repeat thyroid panel. Patient underwent fine needle aspiration (FNA) of the mass which revealed 2018indeterminate follicular neoplasm2019 (Bethesda category IV). The cytologic features were suspicious for neoplastic process, and differential diagnosis was broad including medullary thyroid carcinoma, neuroendocrine tumors, hematology lymphoid process, as well as metastatic malignancy. With concern for malignancy, Positron Emission Tomography 2013 Computed Tomography (PET 2013 CT) scan was done. This revealed intensely hypermetabolic left thyroid mass and mildly hypermetabolic and prominent juxta thyroid lymph nodes in the left neck. Diffuse uptake throughout the remainder of the thyroid gland was present 2013 a common finding associated with Hashimoto2019s thyroiditis. Considering probable malignancy which was thus far undefined, decision for thyroid lobectomy was made. The pathology and immunohistochemical (IHC) stains of the excised left thyroid lobe supported histologic impression of extra nodal marginal B-cell lymphoma (MALT lymphoma) with Hashimoto2019s thyroiditis. IHC indicated positivity for CD20, CD79A, CD43, and CD45. IHC of Superior level 6 lymph node did not reveal any pathologic changes. Bone marrow was performed subsequently which did not show any evidence of infiltrating lymphoma. Patient was determined to be at stage IAE (Ann Arbor staging) considering his disease was limited to the thyroid gland without marrow infiltration, evidence of metastatic disease, or B symptoms. He was started on thyroxine replacement and then referred to Medical and Radiation Oncology, where further radiation therapy was recommended. He remains in a close follow-up with his primary care provider and continues to be in remission. He deferred further radiation therapy.</p>	<p><b>Similarity 1</b> 3582082-1, <b>4196349-1.</b> <b>Relevant</b> 23476858, 34267915, 7985088, 22532918, 11788631, 8838117, 17235456, <b>6193858,</b> <b>25253369,</b> 23714679, 14615444, 24396701, 32071897, 10800981, 29686785.</p>
patient_uid 4196349-1	<p>An 18-year-old boy with 2 years history of UC was referred to our hospital from a clinic for endoscopy. The boy was diagnosed as UC of total colitis type at a large general hospital 2 years earlier. Our hospital performed colonic endoscopy, which revealed erosions, ulcers, and edema continuously from the anus to the cecum. The terminal ileum was not involved. Six biopsies were obtained from various sites of the colorectum. The microscopic examinations of all the six biopsies showed severe infiltration of atypical small lymphocytes [Figure . ]. They showed hyperchromatic nuclei and increased nucleocytoplasmic ratio. Immunoblastic cells were scattered. Centrocyte-like atypical lymphocytes (CCLs), monocytoid cells, and plasma cell differentiations were seen in some places. Vague germinal centers were present, and apparent lymphoepithelial lesions (LELs) were seen [Figure . ]. No crypt abscesses were seen, and there were few neutrophils. No apparent features of UC such as crypt abscess, deletion of goblet cells, abnormal branching of the crypts and cryptal atrophy were seen. No Crohn's granuloma was seen. An immunohistochemical study was performed by the use of Dako Envision method (Dako Corp, Glostrup, Denmark), as previously reported.[ ] Immunohistochemically, the infiltrations were positive for vimentin, CD45, CD20 [ ], CD7903b1 [ ], CD138 [ ], 03ba-chain [ ], 03bb-chain (significantly weaker than 03ba-chain), p53 [ ], and Ki-67 antigen (labeling index = 63%) [ ]. They were also positive for CD45RO, CD3, and CD15, but these positive cells were very scant compared with CD20 and CD7903b1. The infiltrates were negative for CD10, CD30, CD56, cytokeratin (CK) AE1/3, CK CAM5.2, CK34BE12, CK5, CK6, CK7, CK8, CK14, CK18, CK19, CK20, EMA, chromogranin, synaptophysin, NSE, S100 protein, CEA, CA19-9, p63, and HMB45. Without clinical information, the appearances are those of MALT lymphoma. However, with clinical information, making the diagnosis of MALT lymphoma was hesitated. The pathological diagnosis made by the author was atypical lymphoid infiltrates indistinguishable from MALT lymphoma in an adolescent male patient. The patient was planned to be followed up without therapy of MALT but with treatment of UC with salazosulfapyridine and steroids.</p>	<p><b>Similarity 1</b> <b>5901269-1,</b> 4730741-1, 4843722-1. <b>Relevant</b> 23236552, <b>6193858,</b> 23412998, <b>25253369,</b> 29686785, 7883235 ...</p>

Table 11: Samples of PMC-Patients. Id: patient\_uid for note and pubmed\_id for pubmed article. Text: patient note or pubmed title (in bold) and abstract. Annotations: similarity annotations are given by patient\_uid and relevance annotations are given by pubmed\_id. Annotations in red are presented in this table.

Id	Text	Annotations
pubmed_id 6193858	<p><b>Malignant lymphoma of mucosa-associated lymphoid tissue. A distinctive type of B-cell lymphoma</b>            As illustrated in the two cases described in this paper close morphologic and immunohistochemical similarities exist between Mediterranean lymphoma (MTL) and primary gastrointestinal lymphoma of follicle center cell (FCC) origin as it occurs in Western countries. Similarities between the two conditions include a dense noninvasive monotypic lamina propria plasma cell infiltrate, present in all cases of MTL and in some cases of Western gastrointestinal FCC lymphoma, and an invasive infiltrate of FCCs morphologically distinct from the plasma cells. A distinctive lesion produced by individual gland invasion characterizes both types of lymphoma. A clonal relationship between the lamina propria plasma cells and the invasive FCCs, long suspected but never proved in MTL, can be demonstrated in Western cases. Many of the histologic and clinical features common to these lymphomas can be explained in the context of the normal maturation sequences of gut associated lymphoid tissue. It is suggested that MTL and Western cases of primary FCC gastrointestinal lymphoma share a common histogenesis from mucosa associated lymphoid tissue.</p>	-
pubmed_id 25253369	<p><b>Extranodal marginal zone B-cell lymphoma of Mucosa-Associated Lymphoid Tissue (MALT lymphoma) in ulcerative colitis</b>            Extranodal marginal zone B-cell lymphoma of mucosa-associated lymphoid tissue (MALT lymphoma) occurring in inflammatory bowel diseases, including ulcerative colitis (UC) and Crohn's disease, has been reported, although it is extremely rare. An 18-year-old man with a two-years history of UC underwent colon endoscopy, and was found to have active total UC ranging from anus to cecum. Six biopsies were obtained. The microscopic examinations showed severe infiltrations of atypical small lymphocytes. They showed hyperchromatic nuclei and increased nucleocytoplasmic ratio and scattered immunoblastic cells. Centrocyte-like atypical lymphocytes, monocytoid cells, and plasma cells were seen in some places. Vague germinal centers were present, and apparent lymphoepithelial lesions were seen. No crypt abscesses were seen, and there were few neutrophils. No apparent other findings of UC were seen. Immunohistochemically, the atypical lymphocytes were positive for vimentin, CD45, CD20, CD79, CD138, -chain, -chain, and p53 and Ki-67 antigen (labeling index = 63%). They were also positive for CD45RO, CD3, and CD15, but these positive cells were very scant compared with CD20 and CD79. They were negative for CD10, CD30, CD56, cytokeratin (CK) AE1/3, CK CAM5.2, CK34BE12, CK5, CK6, CK7, CK8, CK14, CK18, CK19, CK20, EMA, chromogranin, synaptophysin, NSE, S100 protein, CEA, CA19-9, p63, and HMB45. Without clinical information, the appearances are those of MALT lymphoma. However, with clinical information, making the diagnosis of MALT lymphoma was hesitated. It is only mentioned herein that atypical lymphocytic infiltrations indistinguishable from MALT lymphoma occurred in an 18-year-old male patient with a two-year history of UC.</p>	-